

Enhancement of x-rays generated by a guided laser wakefield accelerator inside capillary tubes

J. Ju, K. Svensson, A. Döpp, H. E. Ferrari, K. Cassou et al.

Citation: *Appl. Phys. Lett.* **100**, 191106 (2012); doi: 10.1063/1.4712594

View online: <http://dx.doi.org/10.1063/1.4712594>

View Table of Contents: <http://apl.aip.org/resource/1/APPLAB/v100/i19>

Published by the [American Institute of Physics](http://www.aip.org).

Additional information on *Appl. Phys. Lett.*

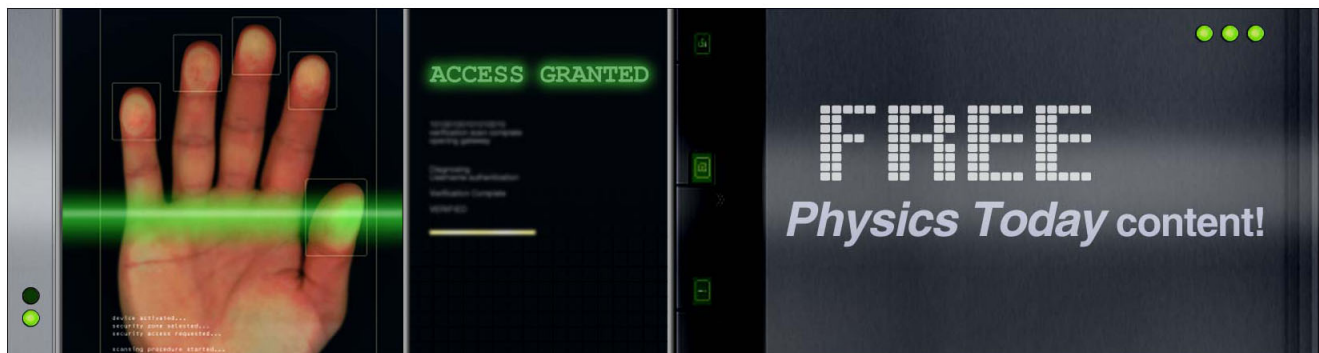
Journal Homepage: <http://apl.aip.org/>

Journal Information: http://apl.aip.org/about/about_the_journal

Top downloads: http://apl.aip.org/features/most_downloaded

Information for Authors: <http://apl.aip.org/authors>

ADVERTISEMENT



Enhancement of x-rays generated by a guided laser wakefield accelerator inside capillary tubes

J. Ju,¹ K. Svensson,² A. Döpp,¹ H. E. Ferrari,³ K. Cassou,¹ O. Neveu,¹ G. Genoud,² F. Wojda,² M. Burza,² A. Persson,² O. Lundh,² C.-G. Wahlström,² and B. Cros^{1,a)}

¹Laboratoire de Physique des Gaz et des Plasmas, CNRS-Université Paris-Sud 11, 91405 Orsay, France

²Department of Physics, Lund University, P.O. Box 118, S-22100 Lund, Sweden

³Consejo Nacional de Investigaciones Científicas y Técnicas (CONICET), 8400 Bariloche, Argentina

(Received 17 January 2012; accepted 24 April 2012; published online 9 May 2012)

Electrons accelerated in the nonlinear regime in a laser wakefield accelerator experience transverse oscillations inside the plasma cavity, giving rise to ultra-short pulsed x-rays, also called the betatron radiation. We show that the fluence of x-ray can be enhanced by more than one order of magnitude when the laser is guided by a 10 mm long capillary tube instead of interacting with a 2 mm gas jet. X-rays with a synchrotron-like spectrum and associated critical energy ~ 5 keV, with a peak brightness of $\sim 1 \times 10^{21}$ ph/s/mm²/mrad²/0.1%BW, were achieved by employing 16 TW laser pulses. © 2012 American Institute of Physics. [<http://dx.doi.org/10.1063/1.4712594>]

Since their discovery, x-rays have contributed to many fields of science and the development of new x-ray sources is an active field of research. Ultra-short x-ray pulses^{1,2} can be generated in a laser wakefield accelerator (LWFA). In the so-called blow-out regime of LWFAs, the ponderomotive force of an intense laser pulse focused in a plasma blows the electrons out of a volume of radius similar to the laser focal spot radius. The charge separation between electrons and ions is associated to electric fields with an amplitude of the order of ~ 100 GV/m. These fields can trap and accelerate longitudinally plasma electrons to high energy, typically 100 MeV, over only a few millimetres, and at the same time wiggle the electrons transversely. The x-ray pulses produced by this mechanism have spectra similar to synchrotron radiation and are often called the betatron radiation. The betatron radiation has intrinsically striking features for ultra-fast imaging: a pulse duration on the femtosecond scale³ and a perfect synchronization to the pump laser.

The use of such x-rays sources for imaging applications has already been demonstrated^{4,5} with photon energies in the range of 1–10 keV and peak brightness of 10^{22} ph/s/mm²/mrad²/0.1%BW. As they are produced by relatively compact laser systems, they have a large potential for dissemination among various user communities. Their development has thus attracted a lot of attention in the past few years, mostly to characterize their properties^{3,6,7} or to control them.^{8,9} Scalings developed for betatron radiation predict that the x-ray photon energy and brightness can be enhanced by increasing the laser intensity or/and decreasing the plasma density.¹⁰ For example, x-rays extending to 50 keV were observed¹¹ by using a peak focused intensity larger than 10^{20} W/cm². The use of laser guiding in capillary tubes has been shown to enable electron acceleration and x-ray emission at low plasma density and low laser intensity.^{12,13}

In this letter, we report on the ability to increase the number of photons produced in the 2–10 keV range by using a lower density, longer plasma inside capillary tubes, compared to the plasma density and length usually achieved with

gas jets. Using 16 TW laser pulses, the generated x-ray peak brightness is multiplied by 30 when the laser beam is guided by a 10 mm long capillary tube instead of using a 2 mm long gas jet.

Experiments were performed at the Lund Laser Centre, Sweden, where a Ti:Sa, 800 nm central wavelength, laser system delivers an energy of up to 1 J in 40 fs full width at half maximum (FWHM) pulses. A deformable mirror is used after compression to compensate for wavefront distortions in the focal plane. The laser beam was focused, using a $f/15$ off-axis parabola, to an Airy-like spot with 19.7 ± 0.8 μm radius at first minimum. With an energy of 650 mJ in the focal plane, the peak intensity was estimated to be $(5.4 \pm 0.1) \times 10^{18}$ W/cm², giving a normalized laser strength parameter $a_0 = 1.6$. Capillary tubes filled with hydrogen gas were used to confine the gas and to partially guide the laser beam. The spectra of electrons accelerated in either a gas jet or capillary tubes were measured by a spectrometer, composed of a 10 cm long permanent magnet, with a central magnetic field of 0.7 T, deflecting the electrons subsequently intercepted by a phosphor screen (Kodak Lanex Regular) imaged onto a CCD camera. Electrons below 42 MeV did not reach the phosphor screen and were not detected. The beam charge was obtained by the absolute calibration of the Lanex screen.¹⁴ X-rays generated by betatron oscillations in the LWFAs were recorded by a x-ray CCD camera placed 110 cm away from the capillary exit on the laser axis, providing a collection angle of 12×12 mrad². The x-ray camera was located outside the vacuum chamber, behind a 300 μm thick beryllium window and a 5 mm air gap. A set of metallic filters (V, Fe, Ni, Sn, and Zr), held together by a 30 μm wire grid, were used in front of the camera to determine the critical energy associated to the x-ray spectrum in the range of 2–10 keV.

Fig. 1 shows the main characteristics of the electrons and x-rays produced inside a 10 mm long, 178 μm diameter capillary tube for two values of the plasma electron density, n_e . The electron energy spectra in (b) and (e) were extracted from the raw Lanex images seen in (a) and (d), respectively, by summing in the vertical direction and rescaling in the horizontal direction to account for magnet dispersion.

^{a)}Electronic mail: brigitte.cros@u-psud.fr.

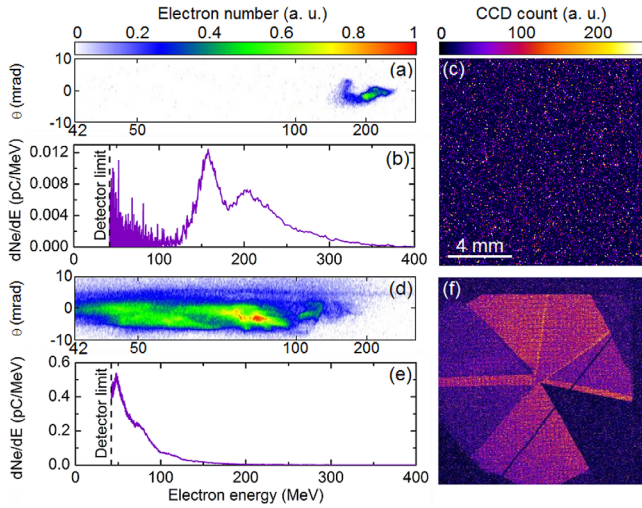


FIG. 1. Single shot raw Lanex images, energy spectra, and x-ray beam images obtained after a 10 mm long, 178 μm diameter capillary tube for two values of the plasma electron density: (a)–(c) $n_e = (5.4 \pm 0.3) \times 10^{18} \text{ cm}^{-3}$; (d)–(f) $n_e = (8.1 \pm 0.5) \times 10^{18} \text{ cm}^{-3}$.

The electron spectra typically exhibit rather large energy spread, and the total charge and maximum energy are strongly dependent on the plasma electron density. The lower density case is close to the density injection threshold¹³ and leads to a maximum energy of the order of 300 MeV (measured at 10% of the maximum of the spectrum), with a low beam charge of 0.9 pC and a divergence FWHM of 5.2 mrad. No x-rays were detected for this shot as seen in Fig. 1(c). At $n_e = (8.1 \pm 0.5) \times 10^{18} \text{ cm}^{-3}$, a 18 pC electron bunch was measured with a maximum energy of ~ 120 MeV, as shown in Fig. 1(e). The corresponding beam divergence is about 5.8 mrad. Fig. 1(f) shows the associated x-ray beam transmitted through the different filters.

The x-ray spectrum can be characterized by a synchrotron-like² spectrum of the form $d^2I/(dE d\Omega)_{\theta=0} \propto (E/E_c)^2 K_{2/3}^2(E/E_c)$, where $K_{2/3}$ is the modified Bessel function of order $2/3$. The critical energy is given by $E_c = 3\hbar K \gamma^2 \omega_\beta$, where $K = \gamma r_\beta \omega_\beta / c$ is the wiggler strength parameter with $\gamma, r_\beta, \omega_\beta$ denoting the relativistic factor, the amplitude, and frequency of betatron oscillation, respectively. The critical energy was evaluated from the transmission of x-rays through the different metal filters with a least squares method.¹¹ In the case of Fig. 1(f), it was found to be 5.4 keV, which is higher than in previous observations^{1,12} with similar laser power.

The maximum x-ray fluence measured is $(5.7 \pm 0.6) \times 10^5 \text{ ph/mrad}^2$ [Fig. 1(f)]. To estimate the peak brightness of this x-ray source, the source size and duration are needed. The source size can be estimated from the expression of critical energy¹⁵ as $r_\beta = E_c c / 3\hbar \gamma^3 \omega_\beta^2$. The relativistic factor is determined using the mean energy of the electron spectra \bar{E}_e , where \bar{E}_e is the average of electron energies weighted by their respective spectral intensities. For the shot plotted in Fig. 1(e), \bar{E}_e is calculated to be 88 ± 4 MeV, and the source size estimated to be $r_\beta = 2 \pm 0.3 \mu\text{m}$. This estimation is validated by 3D simulations performed with the particle-in-cell code CALDER-CIRC,¹⁶ for input parameters close to the experimental ones. They show that the laser pulse non linear evolution in the 178 μm diameter capillary tube leads to a maximum normalized vector potential in the range of $4 < a_0 < 5.5$ and produces accelerated electrons with a mean energy of about 130 MeV. The transverse and longitudinal sizes of the electron bunch in the simulation are 1.3 μm and 10 μm (~ 35 fs), respectively, in reasonable agreement with the estimation from the measurements. The peak brightness achieved in our experiment is estimated, using $r_\beta = 2 \mu\text{m}$, to be $\sim 1 \times 10^{21} \text{ ph/s/mm}^2/\text{mrad}^2/0.1\% \text{ BW}$, and the wiggler strength parameter, $K \simeq 10$. Taking into account the divergence of the x-ray beam, $\theta = K/\gamma$, the estimated total photon number over the whole spectrum is of the order of 10^9 per shot.

The x-ray fluence can be changed by varying the plasma density, as presented in Fig. 2 for two different capillaries. In both cases, the x-ray fluence is maximum for a density of the order of $8 \times 10^{18} \text{ cm}^{-3}$. The influence of the plasma electron density on the x-ray fluence can be understood as a result of the influence of the density on the laser propagation and related electron injection and acceleration. For the parameters of this experiment, at lower densities, electron trapping is not efficient, resulting in a lower beam charge, as seen in Fig. 1. As the plasma density is increased, trapping becomes more efficient and more charge can be accelerated, but the acceleration length and thus the electron energy become smaller due to the shortening of the electron dephasing and laser depletion lengths. For the given laser intensity, the maximum x-ray fluence is achieved in the 10 mm long capillary tube. Simulations in the 178 μm capillary tube for the optimum electron density show that the overall process of laser non-linear evolution, electron injection and acceleration, and x-ray emission occur over the first 10 mm of

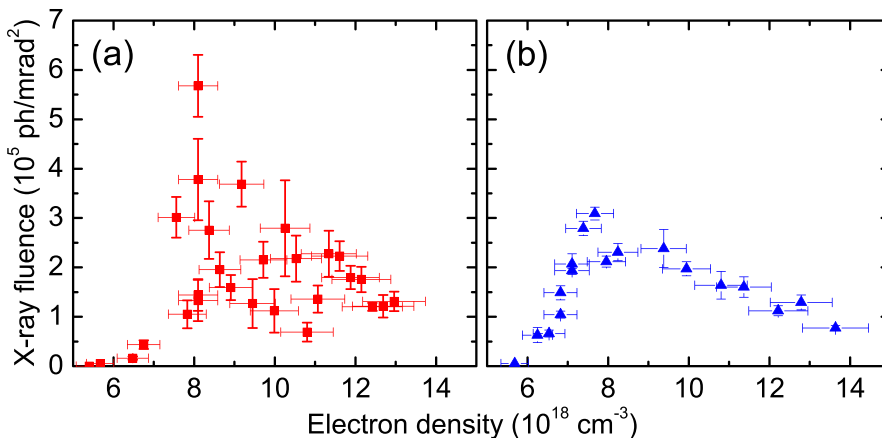


FIG. 2. X-ray fluence as a function of the plasma electron density for (a) a 10 mm long, 178 μm diameter capillary and (b) a 20 mm long, 152 μm diameter capillary; the other parameters are the same as for Fig. 1.

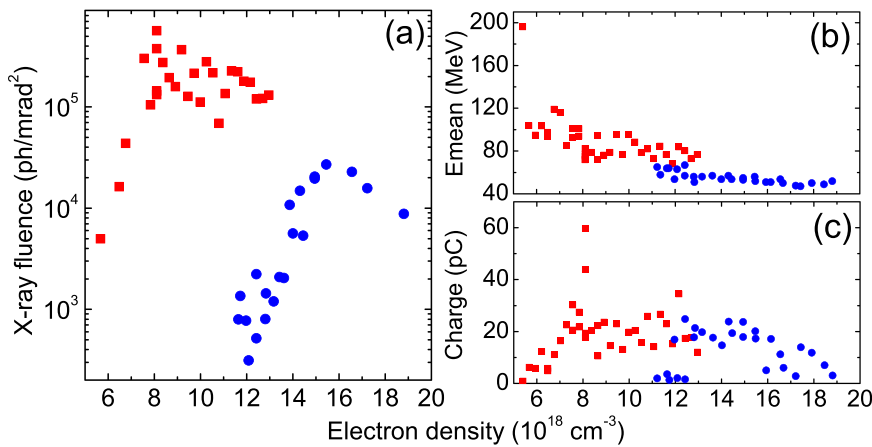


FIG. 3. (a) X-ray fluence, (b) mean energy, and (c) charge of electrons as a function of plasma density for the 10 mm long capillary (red squares) and the 2 mm gas jet (blue dots).

propagation. Fluctuations of the x-ray fluence are smaller at the output of the $152 \mu\text{m}$ diameter, 20 mm long capillary: this can be attributed to the fact that the capillary diameter is smaller favoring a more stable laser guiding. In this case, more x-rays are produced at low densities: it can be due to higher intensities achieved locally inside the capillary, or an evolution of the laser pulse leading to electron injection and acceleration over a distance larger than 10 mm.

The enhancement of the x-ray fluence due to the length and density of the plasma is demonstrated in Fig. 3 by the comparison of the x-ray fluence measured for two targets, 10 mm long capillary tube and 2 mm gas jet, for the same experimental conditions.

It shows that for the intensity used in this experiment, the use of a capillary tube allows electron self-injection to happen at lower density than in the gas jet. The capillary provides a long distance for laser evolution to the threshold required for self-trapping^{12,13} and helps collecting and refocusing the energy initially in the wings of the laser spot;¹⁶ the excitation of multiple modes and their beating can also give rise locally to higher intensity than in vacuum, thus favoring an increase of a_0 . For the gas jet, electron trapping starts around $n_e = 11 \times 10^{18} \text{ cm}^{-3}$, which results in lower energy electrons, as electron energy inversely depends on plasma density. In the intermediate density range of $(11-13) \times 10^{18} \text{ cm}^{-3}$, a higher mean electron energy is achieved when the capillary is employed. The maximum x-ray fluence in the capillary corresponds to the density where the maximum electron charge is measured. The maximum x-ray fluence obtained with the gas jet is $2.7 \times 10^4 \text{ ph/mrad}^2$ for $n_e = 15 \times 10^{18} \text{ cm}^{-3}$. Using the values obtained from experimental data, $E_c = 4.6 \text{ keV}$, $\bar{E}_e = 56 \text{ MeV}$, the source size is estimated to be $2.4 \mu\text{m}$, and the corresponding peak brightness is $\sim 3 \times 10^{19} \text{ ph/s/mm}^2/\text{mrad}^2/0.1\% \text{ BW}$, similar to the result of Ref. 1.

In conclusion, we demonstrate that betatron radiation is significantly enhanced by guiding the laser in a capillary tube allowing electron acceleration in a low density, long plasma. In particular, $\sim 1 \times 10^{21} \text{ ph/s/mm}^2/\text{mrad}^2/0.1\% \text{ BW}$ is the brightest x-ray beam achieved with a $<20 \text{ TW}$ laser. The dependence of the x-ray beam parameters on the capillary tube diameter and length provides additional control of the interaction, and its systematic study will be the subject of future work.

This work was supported by LASERLAB-EUROPE (Grant Agreement No. 228334), the Triangle de la Physique (Grant Agreement NEXT-2009-064 T), the Lund University X-ray Center (LUXC), the Swedish Research Council (including the Linné grant to LLC), and the Knut and Alice Wallenberg Foundation. J. Ju acknowledges financial support from the Chinese Scholarship Council.

¹A. Rousse, K. Ta Phuoc, R. Shah, A. Pukhov, E. Lefebvre, V. Malka, S. Kiselev, F. Burgy, J.-P. Rousseau, D. Umstadter, and D. Hulin, *Phys. Rev. Lett.* **93**, 135005 (2004).

²E. Esarey, B. A. Shadwick, P. Catravas, and W. P. Leemans, *Phys. Rev. E* **65**, 056505 (2002).

³K. Ta phuoc, R. Fitour, A. Tafzi, T. Garl, N. Artemiev, R. Shah, F. Albert, D. Boschetto, A. Rouse, D.-E. Kim, A. Pukhov, V. Seredov, and I. Kostyukov, *Phys. Plasmas* **14**, 080701 (2007).

⁴S. Kneip, C. McGuffey, F. Dollar, M. S. Bloom, V. Chvykov, G. Kalintchenko, K. Krushelnick, A. Maksimchuk, S. P. D. Mangles, T. Matsuoka, Z. Najmudin, C. A. J. Palmer, J. Schreiber, W. Schumaker, A. G. R. Thomas, and V. Yanovsky, *Appl. Phys. Lett.* **99**, 093701 (2011).

⁵S. Fourmaux, S. Corde, K. Ta Phuoc, P. Lassonde, G. Lebrun, S. Payeur, F. Martin, S. Sebban, V. Malka, A. Rouse, and J. C. Kieffer, *Opt. Lett.* **36**, 2426 (2011).

⁶R. C. Shah, F. Albert, K. Ta Phuoc, O. Shevchenko, D. Boschetto, A. Pukhov, S. Kiselev, F. Burgy, J.-P. Rousseau, and A. Rouse, *Phys. Rev. E* **74**, 045401(R) (2006).

⁷S. Fourmaux, S. Corde, K. Ta Phuoc, P. M. Leguay, S. Payeur, P. Lassonde, S. Gnedyuk, G. Lebrun, C. Fourment, V. Malka, S. Sebban, A. Rouse, and J. C. Kieffer, *New J. Phys.* **13**, 033017 (2011).

⁸S. P. D. Mangles, G. Genoud, S. Kneip, M. Burza, K. Cassou, B. Cros, N. P. Dover, C. Kamperidis, Z. Najmudin, A. Persson, J. Schreiber, F. Wojda, and C.-G. Wahlström, *Appl. Phys. Lett.* **95**, 181106 (2009).

⁹K. Ta Phuoc, E. Esarey, V. Leurent, E. Cormier-Michel, C. G. R. Geddes, C. B. Schroeder, A. Rouse, and W. P. Leemans, *Phys. Plasmas* **15**, 063102 (2008).

¹⁰A. G. R. Thomas, *Phys. Plasmas* **17**, 056708 (2010).

¹¹S. Kneip, S. R. Nagel, C. Bellei, N. Bourgeois, A. E. Dangor, A. Gopal, R. Heathcote, S. P. D. Mangles, J. R. Marquès, A. Maksimchuk, P. M. Nilson, K. Ta Phuoc, S. Reed, M. Tzoufras, F. S. Tsung, L. Willingale, W. B. Mori, A. Rouse, K. Krushelnick, and Z. Najmudin, *Phys. Rev. Lett.* **100**, 105006 (2008).

¹²G. Genoud, K. Cassou, F. Wojda, H. E. Ferrari, C. Kamperidis, M. Burza, A. Persson, J. Uhlir, S. Kneip, S. P. D. Mangles, A. Lifschitz, B. Cros, and C.-G. Wahlström, *Appl. Phys. B* **105**, 309 (2011).

¹³H. E. Ferrari, A. F. Lifschitz, G. Maynard, and B. Cros, *Phys. Plasmas* **18**, 083108 (2011).

¹⁴Y. Glinec, J. Faure, A. Guemnie-Tafo, V. Malka, H. Monard, J. P. Larbre, V. De Waele, J. L. Marignier, and M. Mostafavi, *Rev. Sci. Instrum.* **77**, 103301 (2006).

¹⁵F. Albert, R. Shah, K. Ta Phuoc, R. Fitour, F. Burgy, J.-P. Rousseau, A. Tafzi, D. Douillet, T. Lefrou, and A. Rouse, *Phys. Rev. E* **77**, 056402 (2008).

¹⁶H. E. Ferrari, A. Lifschitz, and B. Cros, *Plasma Phys. Controlled Fusion* **53**, 014005 (2011).